

# Stressed State of the Earth's Crust in the Western Region of the Sunda Subduction Zone before the Sumatra–Andaman Earthquake on December 26, 2004

Yu. L. Rebetskii and A. V. Marinin

Presented by Academician S. V. Gol'din August 11, 2005

Received August 11, 2005

DOI: 10.1134/S1028334X06020383

Reconstruction of the parameters of stress tensor based on focal mechanisms of earthquakes occurring before the Sumatra–Andaman earthquake (SAE) showed that deviatoric stresses and all-round compression in the western Sunda subduction zone were distributed nonuniformly. Nonuniform state of the stress in this region is caused by the active sectors of the Andaman–Nicobar and Central Sumatra dextral strike-slip fractures. It was found that peculiarities in the development of the seismic fracture are caused by the revealed inhomogeneity of stresses. The fracture, which originated in the regions with the greatest level of deviatoric stresses and internal elastic energy, spread to the north and south along the subduction zone with different velocities. This is related to different values of the earthquake efficiency during the spreading of the fracture into the region of greater or smaller stresses. The maximal velocity of the development of the fracture front is confined to the lowest stress area, which is located to the north of the fracture initiation. Correspondingly, the epicenter of the earthquake near Nias Island ( $M_w = 8.7$ ) in March 2005 was located to the south of the epicenter of the December 26, 2004, earthquake in the same high stress region.

The SAE on December 26, 2004, was the first earthquake with  $M > 9$  in the epoch of digital seismic observations. The creation of the global network of seismic stations in the mid-1960s, and its increase in subsequent years, made it possible to compile a catalog of earthquake focal mechanisms for all seismogenic regions of the world using the same methods. At present, the Harvard catalog includes more than 40 000 earthquake focal mechanisms with  $M > 4$ . In the early 1970s, E. Carey, J. Angelier, O.I. Gushchenko,

S.L. Yunga, et al., started to develop methods for reconstructing parameters of the tensor of tectonic stresses using seismological data on earthquake focal mechanisms. The uniqueness of the SAE lies in the following fact. The seismological data available in the Harvard catalog allow us to distinguish specific features of the distribution of stresses preceding this strong earthquake over the major part of its source, which extends along the boundary of the subduction of the Indian lithospheric plate under the subcontinental Burma Plate.

The Sumatra–Andaman earthquake occurred at the edge of the Sunda seismic region, which surrounds Sumatra, Nicobar, and the Andaman islands from the west. This part of the Sunda Arc is defined as the region of oblique subduction [1]. Here, the Indian–Australian Plate (azimuth is  $11^\circ$  N) moves to the north at a rate of 6.5 cm/yr, and the Burma Plate slides to the south along the Andaman–Nicobar and Central Sumatra dextral strike-slip fractures. The geodesic data indicate displacements reaching 2.3 cm/yr along the Central Sumatra Fracture. In the Sunda Arc region north of the equator considered here, the oceanic plate has a very flat angle of subduction (approximately  $10^\circ$ ) under the subcontinental plate. South of the beginning of the SAE initiation, the sources of its forerunners were located in the Earth's crust at the contact between the oceanic and subcontinental plates. North of the region, a significantly greater part of the sources were located in the Earth's core of the subcontinental plate. In addition to the subduction zone, pull-apart fractures of the back-arc basin beyond the arch, as well as two large (Andaman–Nicobar and Central Sumatra) dextral strike-slip fractures, served as active seismogenic structures of the subcontinental crust (Fig. 1).

Stresses in the Earth's crust in the western area of the Sunda seismogenic region were reconstructed for the nodes of the  $0.5^\circ$  mesh grid to a depth of 30 km using the cataclastic analysis method [2], using the data on focal mechanisms of 220 earthquakes ( $4.7 < M_b < 6.5$ ) from

Schmidt Joint Institute of Physics of the Earth,  
Russian Academy of Sciences, ul. Bol'shaya Gruzinskaya 10,  
Moscow, 123810 Russia

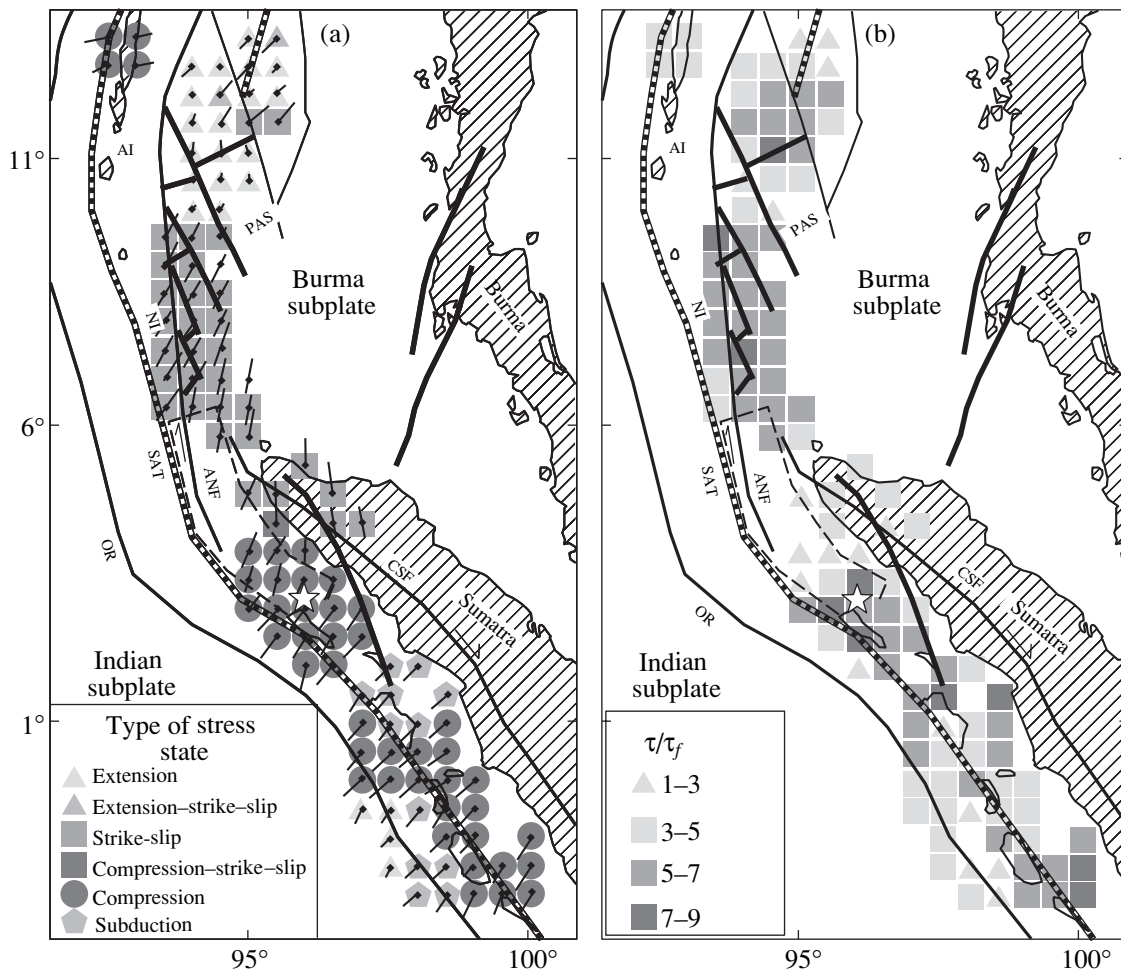


**Fig. 1.** Results of reconstruction natural stresses: (a) orientation of horizontal plane projections of subsidence axes of maximum compression stresses  $\sigma_3$  and type of stressed state; (b) relative values of maximum tangential stress (normalized to internal cohesion of rock massifs). An asterisk indicates the beginning of SAE initiation; dashed segment is the SAE source region near the northern boundary of Sumatra [5]. (CSF) Central Sumatra Fracture; (ANF) Andaman–Nicobar Fracture; (SAT) Sunda–Andaman Trough; (OR) oceanic ridge; (PAS) pull-apart back-arc structures; (AI) Andaman Islands; (NI) Nicobar Islands.

1971 to October 2004 (the data were downloaded from the Harvard University website) [3]. The result of the reconstruction determines the stress tensor parameters with a linear averaging scale of  $\sim 50$  km. The cataclastic analysis of fractures can be considered as a development of the methods for stress reconstruction mentioned above. This method makes it possible to determine not only the orientation of the axes of principal stresses (first stage of the reconstruction), but also to calculate relative values of stresses (second stage). In some cases (third stage), it is possible to estimate the strength of rock massifs, fluid pressure in fissure-pore medium, and absolute values of the stresses.

The analysis of the results of the first stage of reconstruction of stresses that preceded the SAE shows that the Sunda Arc zone was characterized by a sequential change of the stressed state from subduction regime (horizontal compression) in the south to rift regime (horizontal extension) in the north (Fig. 1a). In the subduction region, the axes of maximum deviatoric com-

pression have a gentle slope under the oceanic lithospheric plate (Fig. 1a), while the axes of maximum deviatoric extension steeply dip ( $>45^\circ$ ) under the subcontinental plate. Along the western edge of the Burma Plate, the stress axes of the maximum deviatoric compression and extension become subhorizontal. They are oriented at angles of  $\sim 45^\circ$  to the strike of the Sunda–Andaman Trough. Here, intermediate principal stresses are subvertical. In the northern pull-apart region of the back-arc basin, the axes of maximum compression become subvertical (Fig. 1a). The axes of intermediate principal stress are nearly orthogonal to the strike of the trough axis, while the axes of the maximum deviatoric extension are nearly normal to the strike of the grabens of pull-apart structures.

The subduction regime of the stressed state in the southern Sunda Arc (virtually up to the SAE source opening) is formed in the Earth's crust at the contact between the oceanic and subcontinental lithospheric plates. At the same time, the regime of horizontal exten-

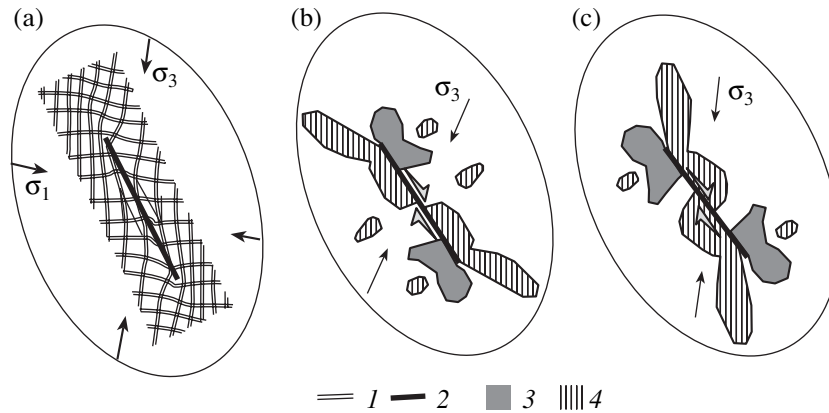


**Fig. 2.** Results of theoretical solution of the strike-slip fracture problem [Osokina, 1987]. (a) Orientation of the axes of principal stresses: (1)  $\sigma_1$ , (2)  $\sigma_3$ ; (b) regions of (3) decrease and (4) increase in maximum tangential stresses relative to the regional state (observed before the activation of the fracture) for values of the angle between the axis of maximum regional compression and fracture plane equal to (b)  $30^\circ$  and (c)  $60^\circ$ .

sion in the back-arc basin and the strike-slip regime at the western boundary of the Burma Plate are formed in the Earth's crust of the subcontinental lithosphere. It is absolutely clear that such sequential transformation of the stressed state from subduction to strike-slip and rift regimes is determined by the motion of the Burma Plate from the north-northwest to the south-southeast. The motion of this plate determines the dextral strike-slip kinematics of the Andaman–Nicobar and Central Sumatra fractures and peculiarities of the stressed state in the continental part of the Earth's crust.

The orientation of the axes of principal stresses at the western flank of the Burma Plate from the SAE source opening to the back-arc basin corresponds well to the orientation of these stresses obtained from the results of the theoretical solution of the problem of strike-slip fractures [4] (Fig. 2a). Note that the deviation of the orientation of the principal axes of stress in this solution is caused by the strike-slip along a solitary fracture, whereas the study region includes two large (Andaman–Nicobar and Central Sumatra) dextral strike-slip fractures, the motion along which is responsible for the pattern of the modern field of tectonic stresses.

An estimate of relative values of stresses (normalized to internal cohesion of rock massifs  $\tau_c$ ) obtained at the second stage of reconstruction showed inhomogeneous distribution of maximum tangential stresses along the arc segment studied here (Fig. 1b). First of all, we distinguish a region of low stresses near the northern boundary of the Sumatra Fracture (approximately 250–300 km long), bordered on both sides by regions of stresses three to four times higher. The place of the SAE source opening (denoted by an asterisk in Fig. 1) was located in the ~250-km-long region of high deviatoric stresses near the boundary with the low stress region (in the zone of maximum stress gradient). While speaking about different stress levels, we note that,

according to the ideology of the cataclastic analysis method, the state of the Earth's crust (with sufficient data on earthquake focal mechanisms for the reconstruction of stresses) is limiting when the Mohr circle is tangent to the external envelope curve, which determines the internal strength of rock massifs.

The appearance of the regions of increased and decreased values of deviatoric stresses, as well as changes in the orientation of the axes of principal stresses, is caused by active parts of the largest dextral strike-slip fractures in the study region. This is evident from the comparison of the results of the reconstruction with the theoretical solution (Figs. 2b, 2c). One can see that the regions of increased maximum shear stresses in the back-arc basin and near the SAE fracture opening correspond to the regions of this type obtained in [4] for the case when the axes of regional stresses of maximum compression are inclined to the strike of the strike-slip fracture at an angle of  $\sim 60^\circ$ . In this case, the high stress regions are located in the extension sectors, which serve as the origin of material transport during the strike-slip. At a steeper angle (approximately  $30^\circ$ ), the high stress regions should be located in the compression sectors, to which the material transport is directed. This case (Fig. 2c) of the distribution of stresses does not correspond to the results of reconstruction.

The theoretical solution presented in Fig. 2b determines the appearance of low stresses (relative to the regional level) in the central part of the strike-slip fracture. The ~300-km-long region of low stresses near the northern boundary of Sumatra (Fig. 1b) should be identified precisely with this area. The high stress region near the SAE source opening and eastern pull-apart structures corresponds to the orthogonal sectors near the terminations of the strike-slip fracture (Fig. 2b), i.e., to such regions, where the axes of maximum compression tend to become orthogonal to its plane. Thus, the southern part of the Andaman–Nicobar Fracture and the northern part of the Central Sumatra Fracture

should be considered a single modern active strike-slip structure, which perturbs the tectonic stress field and forms the stressed state characterized by heterogeneity of all parameters in the western part of the Sunda Arc. The margins of the strike-slip structure are represented by the northeastern part of the back-arc pull-apart structures and the region near the SAE source opening.

The relative  $\frac{\tau}{\tau_f}$  value in the study region varies from 1 to 9. In order to pass from relative to absolute values of stresses at the third stage, it is necessary to estimate the mean effective cohesion  $\tau_f$  for the given scale level from additional provisions (data). This value should be lower than the values obtained from laboratory tests (0.5–1 kbar). As an additional equation for the calculation of  $\tau_f$ , we used the following expression for stresses released in the earthquake source [2]:

$$\frac{\Delta\tau_n}{\tau_f} = 1 - (k_s - k_k) \frac{\sigma_{nn}^*}{\tau_f}, \quad (1)$$

where  $\sigma_{nn}^*$  are effective (with account of the fluid pressure) stresses normal to the fracture, whose values, to the accuracy of normalization by the  $\tau_f$  value, were determined after the first and second stages of reconstruction, and  $k_s$  and  $k_k$  are static and kinematical coefficients of friction, respectively. According to the results of the first stage of reconstruction (based on the analysis of the Mohr diagram) of the distribution of points corresponding to stress vectors on fracture planes in the earthquake sources, the static coefficient was assumed equal to 0.5. According to (1), using the results of the first two stages of reconstruction and assuming  $k_k \leq k_s$  ( $k_k = 0.4$  in the calculations henceforth), we can calculate the  $\Delta\tau_n$  values to the accuracy of normalization by unknown  $\tau_f$  value.

On the other hand, the  $\Delta\tau_n$  values can be estimated using data on the seismic moment  $M_0$  of the SAE and source parameters:

$$\Delta\tau_n = 0.8M_0L_q^2W_q^{-1}, \quad (2)$$

where  $L_q$  and  $W_q$  are the length and width of the source, respectively. The longest segment of the source was used to estimate  $\tau_f$  [5] (Fig. 1a), which made the largest contribution to the seismic energy of the earthquake ( $M_0 = 4 \cdot 10^{22}$  N · m at  $L_q = 420$  km and  $W_q = 240$  km). The data from 12 stress reconstruction nodes, which fall into the region highlighted in Fig. 1a by dashed lines, allowed us to calculate the mean  $\frac{\Delta\tau_n}{\tau_f}$  value for

this region from Eq. (1). Using the value  $\Delta\tau_n \approx 9$  bar (0.9 MPa) and calculating according to (2), we obtain  $\tau_f \approx 35$  bar.

According to the results obtained for the Sunda seismoactive zone, values of the maximum tangential stresses  $\tau$  do not exceed 300–350 bar. Since the strength of brittle rocks in the fracture zones is determined by the Coulomb law, the effective all-around pressure of  $p^*$  (tectonic pressure after subtracting fluid pressure) correlates with the maximum tangential stresses [6]. The calculations showed that the studied segment of the Sunda Arc is characterized by  $\frac{p^*}{\tau} = 0.87$ –2.10. Thus,

regions with a high level of deviatoric stresses are also characterized by high values of the effective pressure, which are responsible for the existence of intense friction forces on the planes of activated fractures.

The data on parameters of the stress tensor are reflected in specific features of the SAE source spreading, as well as in the intensity and velocity of relative displacement of its shores. Analysis of seismic records in [7] showed that during the first 50 s, the fracture propagated with a relatively low velocity ( $\sim 2$  km/s) from a depth of 30 km to the surface and in the north-western direction at a low intensity of seismic radiation [8], resulting in a small amplitude of displacements (less than 3 m). According to the analysis performed above, this initial 100-km-long segment is located in the region of high deviatoric stresses (Fig. 1b) and stresses normal to the fracture. In [6], we showed that friction forces in such regions lead to a transition of the major portion of the released elastic energy into heat. In the limiting case, when the entire released energy is transformed into heat, the fracture develops as a creep. Thus, we can suppose that the observed low velocity of fracture propagation at this stage is related to high tensions in this region.

In the next segment, the velocity of fracture front drastically increased from south to north (up to 3 km/s). The fracture segment near the northern boundary of Sumatra (320–350 km long) is characterized by the greatest displacements (up to 20 m) and a magnitude of  $M_w \approx 9$  [8]. We believe that the large velocity of the fracture front in this segment is caused by a low level of friction forces (as is evident from Fig. 1b, the region of lowest deviatoric stresses and stresses normal to the stress fracture is located here), which provide a high efficiency of the earthquake (ratio of the energy of seismic waves to the entire released energy). Together with the next 320-km-long Nicobar segment of the fracture, this segment served as the tsunami source during the SAE. As compared to the initial segment, the Nicobar segment is characterized not only by a similar (i.e., very high) level of stresses (Fig. 1b), which are similar to those in the initial segment, but also by a relatively high level of seismic wave energy. This can be related to the influence of inertia forces, which made it possible to overcome the high level of friction forces over this segment owing to the dynamic development of the fracture.

The SAE source originated at the contact between the regions with different values of deviatoric stresses and spread into these regions with different velocities. Rock massifs in these regions, which can be considered as conjugated hard (high stresses) and soft (low stresses) inclusions [9], are located in the limiting state (according to the Coulomb law). However, efficiency of the transition of energy accumulated in elastic deformations into the energy of seismic waves is different in these regions. Therefore, the fracture front propagating to the north into the lower stress region had the maximal velocity of development. The velocity of the southern fracture front, which developed in the high stress region, was close to the creep velocity in the higher friction region. We suppose that the hypocenter of the March 2005 earthquake near Nias Island ( $M_w = 8.7$ ) was located in the creep region of the source. Therefore, the event can be considered an aftershock of the SAE.

The fact of the occurrence of a strong earthquake in the stress field of inhomogeneous intensity compels us to revise the currently existing concepts on the process of earthquake preparation [10]. According to these concepts, tangential stresses increase up to the limiting value in the future earthquake region, and the aftershock activity is accompanied by the relaxation of stresses in specific source zones, where the stresses remained high even after the earthquake. Results of the reconstruction of SAE stresses suggest the following assumption. The presence of a high stress gradient zone and elongated region, which is located in the critical but low stress state, is one of the crucial factors responsible for the occurrence of an earthquake with energy drasti-

cally exceeding the energy of the major (strong) events in a seismoactive region of the Earth's crust.

#### ACKNOWLEDGMENTS

This work was supported by the Russian Foundation for Basic Research, projects nos. 03-05-64709, 03-05-64998, and 03-05-65092.

#### REFERENCES

1. V. E. Khain, and M. G. Lomidze, *Geotectonics with Principles of Geodynamics* (MGU, Moscow, 1995) [in Russian].
2. Yu. L. Rebetskii, Doctoral Dissertation in Physics and Mathematics (Moscow, 2003).
3. Yu. L. Rebetskii and A. V. Marinin, in *The Seventh Geophysical Lectures in Memory of V.V. Fedynskii (March 3–5, 2005)* (Moscow, 2005) [in Russian].
4. D. N. Osokina, *Stress and Strain Fields in the Earth's Crust* (Nauka, Moscow, 1987), pp. 120–135 [in Russian].
5. R. Bilham, *Science* **308**, 1125 (2005).
6. Yu. L. Rebetskii, *Dilatancy, Porous Pressure of Fluid, and New Data on the Strength of Rocks in Natural State* (Nauka, Moscow, 2005).
7. C. J. Ammon, C. Ji, H.-K. Thio, et al., *Science* **308**, 1133 (2005).
8. T. Lay, H. Kanomory, C. J. Ammon, et al., *Science* **308**, 1127 (2005).
9. I. P. Dobrovolskii, *Theory of Earthquake Source Preparation* (IFZ RAN, Moscow, 1991) [in Russian].
10. V. I. Mjachkin, W. F. Brace, G. A. Sobolev, and J. H. Dieterich, *Pure Appl. Geophys.* **113**, 169 (1975).